

Joint Scalable Coding and Routing for 60 GHz Real-Time Live HD Video Streaming Applications

Joongheon Kim, *Member, IEEE*, Yafei Tian, *Member, IEEE*, Stefan Mangold, *Member, IEEE*, and Andreas F. Molisch, *Fellow, IEEE*

Abstract—Transmission of high-definition (HD) video is a promising application for 60 GHz wireless links, since very high transmission rates (up to several Gbit/s) are possible. In particular we consider a sports stadium broadcasting system where signals from multiple cameras are transmitted to a central location. Due to the high pathloss of 60 GHz radiation over the large distances encountered in this scenario, the use of relays might be required. The current paper analyzes the joint selection of the routes (relays) and the compression rates from the various sources for maximization of the overall video quality. We consider three different scenarios: (i) each source transmits only to one relay and the relay can receive only one data stream, and (ii) each source can transmit only to a single relay, but relays can aggregate streams from different sources and forward to the destination, and (iii) the source can split its data stream into parallel streams, which can be transmitted via different relays to the destination. For each scenario, we derive the mathematical formulations of the optimization problem and re-formulate them as convex mixed-integer programming, which can guarantee optimal solutions. Extensive simulations demonstrate that high-quality transmission is possible for at least ten cameras over distances of 300 m. Furthermore, optimization of the video quality gives results that can significantly outperform algorithms that maximize data rates.

Index Terms—60 GHz, Multi-Gbit/s HD Video Streaming, Wireless Video Quality Maximization, Routing.

I. INTRODUCTION

RECENTLY, wireless data transmission and media streaming in the millimeter-wave frequency range have received a lot of attention by the wireless communications and consumer electronics communities. In particular the 60 GHz frequency range is of great interest: a 7 GHz wide band

Manuscript received June 21, 2012; revised June 11, 2013; accepted July 2, 2013. Date of publication July 30, 2013; date of current version August 21, 2013. The work of J. Kim was supported by a gift from Disney Research. Parts of this paper were presented at the 22nd IEEE International Symposium on Personal Indoor and Mobile Radio Communications, Toronto, Canada, in September 2011, and at the IEEE International Conference on Communications, Budapest, Hungary, in June 2013 (refer to [16] and [29]).

J. Kim is with the Department of Computer Science, University of Southern California, Los Angeles, CA 90089 USA (e-mail: joongheon.kim@usc.edu).

Y. Tian is with the School of Electronics and Information Engineering, Beihang University, Beijing 100191, China (e-mail: ytian@buaa.edu.cn).

S. Mangold is with Disney Research, Zurich 8092, Switzerland (e-mail: stefan@disneyresearch.com).

A. F. Molisch is with the Department of Electrical Engineering, University of Southern California, Los Angeles, CA 90089 USA (e-mail: molisch@usc.edu).

Color versions of one or more of the figures in this paper are available online at <http://ieeexplore.ieee.org>.

Digital Object Identifier 10.1109/TBC.2013.2273598

(58-65 GHz) has been made available for unlicensed operation. This large bandwidth enables multi-Gbit/s wireless data transmission [1], [2], which enables, in turn, high definition (HD) video streaming in an uncompressed, or less compressed, manner. Therefore, several industry consortia such as WirelessHD [3] and the Wireless Gigabit Alliance (WiGig) [4] have developed related technical specifications. Also within the IEEE, there are two 60 GHz millimeter-wave standardization activities, i.e., IEEE 802.15.3c Millimeter Wave Alternative PHY [5] and IEEE 802.11ad Very High Throughput (VHT) [6]. First consumer electronics products for short-range transmission (e.g., from Blue-Ray player to HDTV) have recently become available.

In this paper, we analyze 60 GHz for longer-range outdoor applications, specially an outdoor sports broadcasting system. In this system, there are multiple wireless HD video cameras in a sports stadium for high-quality real-time broadcasting, all sending their data to a single destination (called “broadcasting center”, even though it is the *receiver* of the data streams). To transmit uncompressed HD video streams in real time, a data rate of approximately 1.5 Gbit/s is required¹. Since the distance between wireless HD video cameras and a broadcasting center is on the order of several hundred meters, the high pathloss at 60 GHz is one of the main challenges that leads to a limitation of coverage and/or reduction of the possible data rate. One promising way to deal with this problem is using *relays* to extend the coverage range [7]. Increasing the number of relays obviously improves performance, but also increases costs. We are thus interested in finding the tradeoff between performance and number of relays.

We furthermore take the complexity of the antennas into account. In order to compensate for the high pathloss, as well as to reduce interference, high-gain antennas need to be employed. We distinguish between the situations where the antenna can form only a single beam, or multiple beams: (i) If both source and relay have only a single beam, then each source has to select a suitable relay, and the relay can only receive from this particular source. (ii) If sources have single

¹In a single HD video frame, 1080×1920 pixels exist and each pixel has 24 bit information for RGB format (8 bit for Red, Green and Blue color representation, respectively). In addition, for one second, 30 frames are required in a standard mode. Therefore, approximately 1.5 Gbit/s data rate is required for uncompressed HD video streaming. In addition, for the enhanced mode, 60 frames are required [2]. This paper considers the standard mode but can be extended for the enhanced mode as well.

beams, but relays have multiple beams, then the source can transmit only to a single relay, but the relays can receive data from multiple sources and aggregate them before forwarding to the destination. (iii) If also the source has multiple beams, it can split its data stream into multiple parallel streams and send them to the destination via parallel links. In case (i), some HD video streams from sources cannot be served by the relays if the number of relays is less than the number of sources. In cases (ii) and (iii), appropriate compression and routing of multiple streams via the same relay can be used.

Relay selection for maximization of data throughput has been analyzed in many papers (see Sec. II). However, for video transmission, we are not interested in maximizing the data rate arriving at the destination, but rather the *video quality*, which is related to the data rate in a nonlinear manner. To achieve this goal, the proposed mathematical formulation will select the relays for every single HD video stream and decide the coding (compression) rates for each stream. With this formulation for the three cases, the optimal solutions can be obtained by (i) the theory of unimodular matrices, (ii) a BBLP algorithm [8], or (iii) standard convex optimization techniques.

The remainder of this paper is organized as follows: Section II gives an overview of related work. Section III explains the details of our reference system. Section IV presents the details of the joint scalable video coding and relaying algorithms for maximizing the delivered HD video qualities for the three cases. Section V presents the technique to convert the mathematical optimization framework of Section IV to a convex form, which can guarantee optimal solutions. Section VI evaluates the performance and Section VII concludes this paper.

II. RELATED WORK

The topic of wireless network technologies for outdoor sports stadium system was discussed in [9]; however the fundamental setup differs from ours in that [9] considers content distribution to wireless devices of the audience in the stadium, while our investigations are for the real-time streaming service to a broadcasting center in the stadium and from there to audiences at home. In terms of fundamental technology, our research is related to both scalable video coding rate control and relay selection/routing for real-time video transmission.

For the video relaying issue, example publications include [10], [11], [12], [13]. The proposed scheme in [10] addresses opportunistic routing for video transmission over IEEE 802.11 wireless networks under given time constraints. The proposed scheme is efficient in the given multi-hop IEEE 802.11 wireless networks, however, it does not consider the route paths selection problem. Ref. [11] considers distributed video streaming in multi-hop wireless networks. This paper considers network architectures similar to ours (when specialized to the two-hop case), but the proposed algorithm cannot consider the rate control mechanism. The formulation in [12] considers multipath selection for video streaming in a mobile ad-hoc network (MANET) architecture. The main

constraint for this algorithm is the interference over the given wireless channel, a factor that does not play a role in our 60 GHz millimeter-wave wireless channel, where the high directionality of the antennas prevents inter-stream interference. The scheme in [13] considers a route selection mechanism for video streaming, but using multipath video streaming with multicast techniques, which differs from our setup where only a single destination is used. All of these papers [10], [11], [12], [13] only consider the video multi-hop wireless networks but do not consider the video coding rate control. For the same reason, the rich literature of relay selection and routing of “conventional” data transmission is not applicable to our scenario. In previous research on video streaming, schemes usually considered multipath video data transmission to combat the limited wireless bandwidth [11], [12], [13]. In addition, some of the research considered retransmission of video signals and tried to reduce transmission time [10]. However, thanks to the very large available bandwidth at 60 GHz, these factors are not considered in this paper.

A representative work which considers both rate control and route selection appeared in [14]: the proposed algorithm selects the best relays for individual unicast data flows and it selects the corresponding data rates as well. However, the relays in [14] cannot aggregate video streams, which is required when the number of relays is smaller than the number of unicast flows in real-time video streaming applications. In addition, the proposed framework does not consider the properties of video, namely the nonlinear relationship between data rate and video quality because it is for generalized cooperative multi-hop networking systems. In addition, the algorithms in [10], [11], [12], [13], [14] do not consider the features of millimeter-wave wireless channels; in particular, they do not consider beamforming for interference suppression, which is an essential part of our architecture. Ref. [15] considers the main features of millimeter-wave wireless communications, i.e., high directionality. It designs the medium access control mechanisms for 60 GHz wireless channels, however, it does not consider the features related to video streaming. In [16], we considered the properties of the 60 GHz channel as well as rate control and video quality, but we restricted ourselves to the case that the number of relays exceeds the number of sources. This comparison is summarized in Table I. In a conference version of our work [29], *per-link* quality is considered instead of *per-source* quality consideration. Considering per-link quality is meaningful when multiple streams emanate from one source location, each being transmitted via one link. If, as assumed in this paper, each source creates one video stream, considering the quality of each source is the most meaningful consideration.

III. A REFERENCE SYSTEM MODEL

A. Link Budget Analysis: Capacity Perspective

A link budget analysis [17] provides the fundamental trade-off between data rate and range that can be achieved. Using Shannon’s equation for the capacity

$$C = B \cdot \log_2(1 + \text{SNR}) \quad (1)$$

TABLE I
RELATED WORK COMPARISON TABLE

Consideration Factors	[10]	[11]	[12]	[13]	[14]	[16]	Proposed
Route Selection	○	○	○	○	○	○	○
Rate Allocation	×	×	×	×	○	○	○
Millimeter-Wave Channels	×	×	×	×	×	○	○
Multiple-Antenna Elements	×	×	×	×	×	×	○
Video Streaming	○	○	○	○	×	○	○
Insufficient Number of Relays	-	-	-	-	-	×	○

where SNR is equal to $P_{\text{signal}}/P_{\text{noise}}$ as a linear scale, P_{signal} and P_{noise} stand for the signal power and noise power, respectively. In addition, B stands for bandwidth and is considered as 2.16 GHz following WiGig specification [6]. The signal power expressed in dB, $P_{\text{signal,dB}}$, can be computed as follows:

$$P_{\text{signal,dB}} = E + G_r - W - O(d) + F(d) \quad (2)$$

where E stands for the equivalent isotropically radiated power (EIRP), which is limited by frequency regulators to 40 dBm in the USA and 57 dBm in Europe. G_r means the receiver antenna gain; In our system it is set to 40 dB, which corresponds to commercial high-gain 60 GHz outdoor scalar horn antennas [18], [19], which we propose to achieve large communication range. W presents the shadowing margin and is set to 10 dB; while line-of-sight (LOS) is anticipated for our deployment, obstacles such as passing-by people, raised banners, etc., might attenuate the LOS. $F(d)$ represents the path loss, which depends on the distance (in meter) d between transmitter and receiver

$$F(d) = 10 \log_{10} \left(\frac{\lambda}{4\pi d} \right)^n \quad (3)$$

where n stands for the path loss coefficient and is set as 2.5 [1]. In addition, the wavelength (λ) is 5 millimeter at 60 GHz. $O(d)$ means the oxygen attenuation at d , which can be computed as $O(d) = \frac{15}{1000}d$. For $d < 200$ meter, $O(d)$ can be ignored [1]. The noise power in dB, $P_{\text{noise,dB}}$ can be computed as follows:

$$P_{\text{noise,dB}} = 10 \log_{10} (k_B T_e \cdot B) + F_N \quad (4)$$

where $k_B T_e$ stands for the noise power spectral density which is -174 dBm/Hz and F_N is the noise figure of the receiver and set as 6 dB.

This leads us to conclude that approximately 200 – 300 m is the maximum distance for successful signal decoding when the maximum rate of 1.5 Gbit/s is used, as shown in Fig. 1.

B. Outdoor Broadcasting Systems with 60 GHz Wireless Links

It follows from the above link budget that the assistance of relays is required if the wireless communication range between wireless HD video cameras and a single broadcasting center is more than 200 – 300 m. In the general transport layer mechanisms such as TCP, the congestion control mechanism encounters a number of new problems and suffers from poor performance in multi-hop wireless networks [20]. Thus, considering a small number of hops is beneficial. Furthermore, the size of sport stadium (i.e., from wireless HD video cameras to the antennas of a broadcasting center) is not more than 500 m,

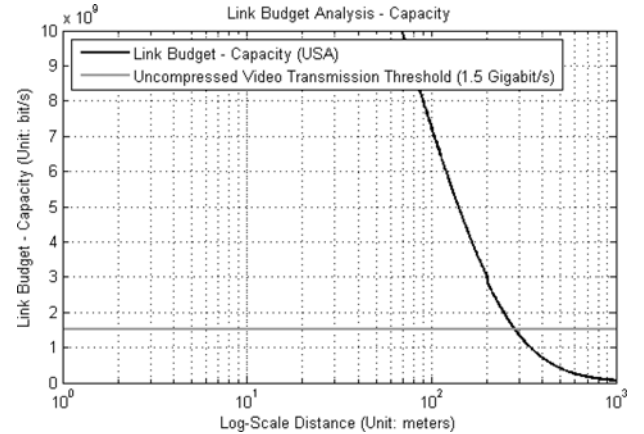


Fig. 1. Link Budget Analysis: Capacity (Unit: bit/s) vs. Log-Scale Distance (Unit: meters).

e.g., the large side of Los Angeles Memorial Coliseum is approximately 300 m. Thus, we can safely restrict the number of relays to one, i.e., a two-hop network.

In our outdoor sports broadcasting system, mainly three components with 60 GHz wireless communication capabilities are relevant, i.e., wireless HD video cameras, relays, and a broadcasting center using multiple antennas. As presented in Fig. 2(a), the proposed wireless HD video cameras have scalable video coding (SVC) functionalities that reproduce the real-world analog video signals as layered SVC-coded HD video bit streams. If the achievable rate of a 60 GHz link is sufficient for uncompressed HD video streaming (i.e., 1.5 Gbit/s), then all SVC-coded layers can be transmitted, i.e., the optimal coding level decision module selects all layers. Hence, this can preserve the maximum quality of the delivered video streams. This achievable rate between x and y ($\mathcal{A}_{x \rightarrow y}$) is computed by (1). If the computed achievable rate is not enough for uncompressed HD video streaming (i.e., less than 1.5 Gbit/s), the optimal coding level decision module has to determine the maximum number of layers, reducing the overall video quality (see below) as discussed in [21], [22].

Each wireless HD video camera can have one of two antenna types: single-beam antennas, or multiple-beam antennas. Single-beam antennas usually are high-gain antenna structures such as horn antennas or Cassegrain antennas. In the scenario with single-beam antennas at the sources, all the multiple SVC-coded streams in each camera are assigned to the single antenna, and thus transmitted to the same relay. If the antenna can form N independent beams the multiple SVC-coded streams are divided into N parts and each part is

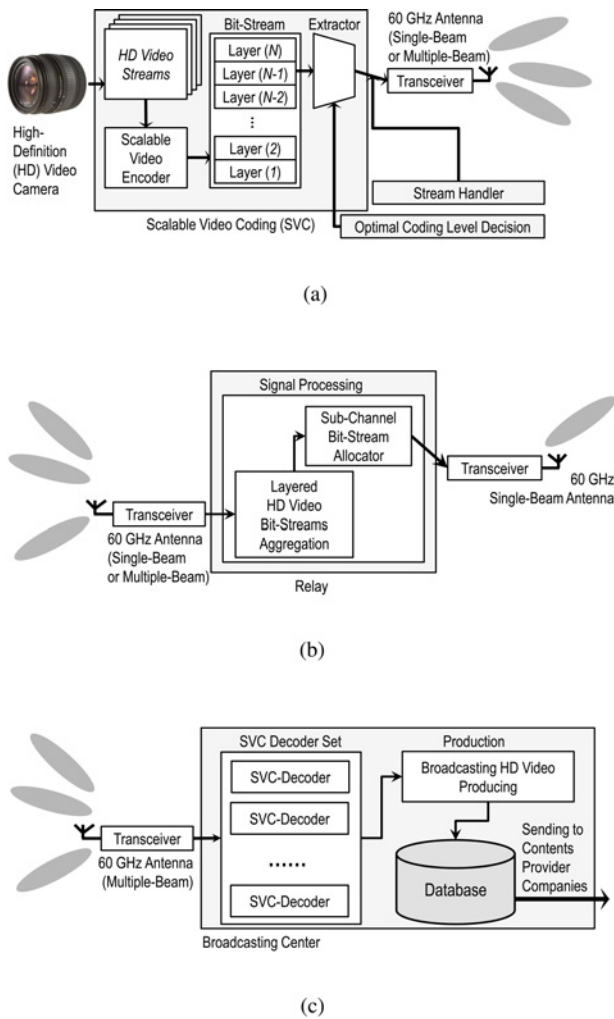


Fig. 2. System Components, (a) Wireless HD Video Camera (Source) Structure, (b) Relay Structure, (c) Broadcasting Center Structure.

assigned to a beam to be concurrently transmitted. Normally, the multiple beams will be formed by phased-array type antennas, though the use of multiple horn antennas pointing into different directions is possible as well.

If the number of sources exceeds the number of relays, the relays have to have multiple-beam antennas for reception. If the number of sources is smaller than the number of relays, single-beam antennas might be sufficient. In either case, the number of beams for transmission to the broadcast center need not exceed one, since there is only one destination. The destination, however, always has to be able to receive multiple beams simultaneously. Fig. 2(b) shows the proposed architecture when the relays have multiple-beam antennas. The relays use their built-in digital signal processing unit to aggregate the received HD video signals and transmit them towards a broadcasting center via the single antenna. We assume that the used relay in this system is an ideal decode-and-forward relay with zero latency. As presented in Fig. 2(c), the proposed broadcasting center has multiple antennas which are facing the relays. We emphasize that due to the narrow beamwidth (1.5-10° [18], [19]), of the antennas, multiple streams arriving at the broadcast center do

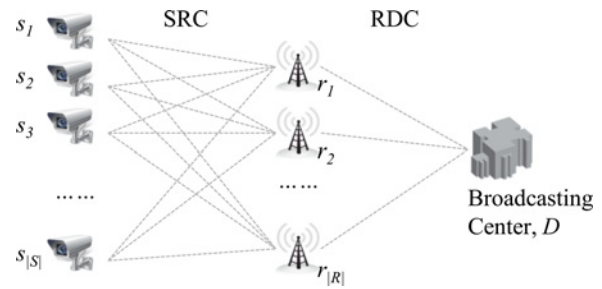


Fig. 3. A System Model: SRC and RDC stand for the “Source-Relay Combination” and “Relay-Destination Combination,” respectively.

not interfere with each other (and similarly for the relays). This broadcasting center selects important features of the current real-time sports game. For interactive TV where users can select the camera/viewpoint they prefer, it is often desirable to maximize the overall video quality, subject to constraints on the minimum acceptable quality for each video stream.

IV. JOINT SCALABLE CODING AND ROUTING

Fig. 3 shows the system model with a set of sources \mathcal{S} , a set of relays \mathcal{R} , and a single destination. In the relay-destination combination (RDC) part of Fig. 3, all relays (i.e., $r_1, \dots, r_{|\mathcal{R}|}$) are connected to the single destination (i.e., the broadcasting center D). Then the maximum achievable rates of all possible relay-destination pairs are computed (denoted as $a_{r_1 \rightarrow D}^{\text{RDC}}, \dots, a_{r_{|\mathcal{R}|} \rightarrow D}^{\text{RDC}}$). We assume that the destination can form a sufficient number of independent beams so that it has no limitations concerning the number of relays from which it can receive. Thus, finding optimal combinations between sources and relays in SRC are considered for the following three scenarios: (i) sources and relays have only a single beam (Sec. IV-A), (ii) sources have single beams and relays have multiple beams (Sec. IV-B), and (iii) both sources and relays can form multiple beams (Sec. IV-C).

For all possible scenarios, our objective is the maximization of the sum of the overall video qualities delivered to the destination. As a first step, the relationship between the video qualities and data rates should be defined. The quality of HD video signals is related to the data rate in a nonlinear and monotonically increasing form, e.g., logarithmically. One widely suggested model [23], [24], [25] which is applicable to H.264/MPEG4 AVC, is presented in Fig. 4. In addition, there is no compression loss if the data rate is more than 1.5 Gbit/s because we can exploit uncompressed HD video transmission in a standard mode as shown in Fig. 4. We note, however, that this figure might depend on the type of video source - e.g., will be different for fast-moving and slow-moving video. The main feature we include in our modeling are a monotonic, but sublinear, increase of video quality with data rate.

A. Single-Beam Antennas at Sources and Relays

Each source has a single-beam antenna and thus can send only to one relay, in addition, each relay also has a single-beam antenna for receiving data. Our objective is the maximization

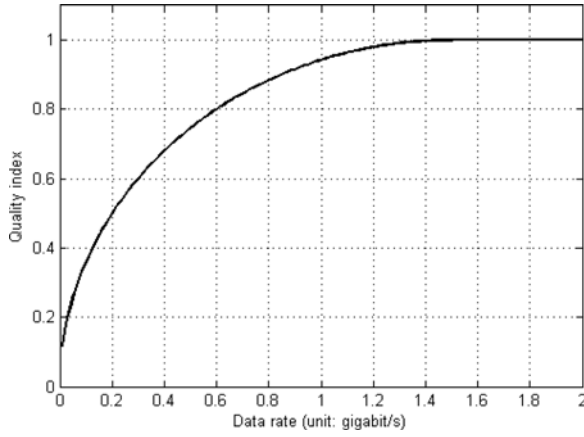


Fig. 4. Generalized relationship between the quality index of transmitted HD video signals and data rates. Based on different kinds of HD video sources, the curve can be varied, but the general form is given as logarithmically and monotonically increasing as proved in [23], [24], [25].

of the sum of video qualities delivered from sources to the destination:

$$\max : \sum_{i=1}^{|\mathcal{S}|} f_q \left(\sum_{j=1}^{|\mathcal{R}|} \frac{1}{2} a_{s_i \rightarrow r_j}^{\text{SRC}} x_{s_i \rightarrow r_j}^{\text{SRC}} \right) \quad (5)$$

subject to

$$\sum_{i=1}^{|\mathcal{S}|} a_{s_i \rightarrow r_j}^{\text{SRC}} x_{s_i \rightarrow r_j}^{\text{SRC}} \leq \mathcal{A}_{r_j \rightarrow D}^{\text{RDC}}, \forall j, \quad (6)$$

$$\sum_{i=1}^{|\mathcal{S}|} x_{s_i \rightarrow r_j}^{\text{SRC}} \leq 1, \forall j, \quad (7)$$

$$\sum_{j=1}^{|\mathcal{R}|} x_{s_i \rightarrow r_j}^{\text{SRC}} \leq 1, \forall i, \quad (8)$$

$$a_{s_i} \leq \sum_{j=1}^{|\mathcal{R}|} a_{s_i \rightarrow r_j}^{\text{SRC}} x_{s_i \rightarrow r_j}^{\text{SRC}}, \forall i, \quad (9)$$

$$a_{s_i \rightarrow r_j}^{\text{SRC}} \leq \mathcal{A}_{s_i \rightarrow r_j}^{\text{SRC}}, \forall i, \forall j, \quad (10)$$

$$x_{s_i \rightarrow r_j}^{\text{SRC}} \in \{0, 1\}, \forall i, \forall j, \quad (11)$$

$$x_{r_j \rightarrow D}^{\text{RDC}} = 1, \forall j. \quad (12)$$

In this formulation, i and j are the indices of sources and relays where $i \in \{1, \dots, |\mathcal{S}|\}$ and $j \in \{1, \dots, |\mathcal{R}|\}$ where \mathcal{S} and \mathcal{R} stand for the sets of sources and relays, respectively. If the connection between s_i and r_j is active (i.e., if source s_i selects relay r_j), then the binary index variable $x_{s_i \rightarrow r_j}^{\text{SRC}}$ is 1 by (11); otherwise it is 0 by (11). The given relays should be connected to the destination D , thus, $x_{r_j \rightarrow D}^{\text{RDC}} = 1$ by (12). The $\mathcal{A}_{s_i \rightarrow r_j}^{\text{SRC}}$ and $\mathcal{A}_{r_j \rightarrow D}^{\text{RDC}}$ are maximum achievable rates for the corresponding wireless links and computed by (1). In addition, the desired data rates between s_i and r_j , i.e., $a_{s_i \rightarrow r_j}^{\text{SRC}}$, should be less than or equal to the computed $\mathcal{A}_{s_i \rightarrow r_j}^{\text{SRC}}$ as shown in (10). As shown in (9), we have to achieve the required minimum data rates for each flow (i.e., a_{s_i} , $\forall s_i$) to guarantee the required minimum video qualities for each flow (i.e., $f_q(a_{s_i})$, $\forall s_i$) where $f_q(\cdot)$ is a function for the relationship between video quality and data rate (refer to Fig. 4). In addition, $\mathcal{A}_{s_i \rightarrow r_j}^{\text{SRC}}$ from s_i to r_j and $\mathcal{A}_{r_j \rightarrow D}^{\text{RDC}}$ from r_j to D are fixed values because the sources and relays are not mobile and the channel is not time-varying.

Since each relay can receive one video stream, and these have to go to the destination via the wireless link with a limited

capacity $\mathcal{A}_{r_j \rightarrow D}^{\text{RDC}}$, (6) follows. For each individual source, there is at most one outgoing flow toward relays because the sources have single-beam antennas, as formulated in (8). Similarly, each relay can form only one beam in receiving mode, thus the number of incoming flows from sources can be at most one as formulated in (7). Finally, (5) describes the objective of finding the set of pairs between sources and relays as well as finding the corresponding data rates for maximizing the total video quality and the corresponding data rate value becomes half due to half-duplex constraint.

The set of equations (5 - 12) can be solved by the method of Sec. V. Alternatively, we note that this setup is a special case of a scenario treated in our conference paper [16]. In that paper, the proposed algorithm addresses the relay selection and cooperative communication scheme selection for a situation where several source-destination unicast pairs exist, and furthermore transmission between the pairs can occur not only using decode-and-forward, but also amplify-and-forward (AF), and non-cooperative communications (non-CC) direct transmission. In the system configuration of [16], an algorithm selects the relay node and transmission mode for every single unicast pair in terms of maximization of overall transferred video qualities. Thus, our mathematical formulation, which shows that the connectivity matrix is totally unimodular, which in turn guarantees polynomial-time solutions (i.e., a closed-form solution is possible), can be applied also in this case. On the other hand, this framework cannot be easily generalized to the multi-beam scenarios.

The proposed scheme in this section is meaningful under the assumption that the number of relays is larger than or equal to the number of sources; otherwise, some video flows from sources cannot reach to the destination. However, positioning many relays obviously increases the cost of the network. To deal with this problem, more advanced relay architectures, which allow multiple-beam antennas, are proposed and the schemes for this case are discussed in the following two sections.

B. Single-Beam Antennas at Sources and Multiple-Beam Antennas at Relays

Each source has a single-beam antenna and thus can send only to one relay, while relays can aggregate streams from different sources. Therefore, the relays have multiple-beam antennas, the constraint (7) is updated to allow multiple incoming flows as follows:

$$\sum_{i=1}^{|\mathcal{S}|} x_{s_i \rightarrow r_j}^{\text{SRC}} \leq B_{r_j}, \forall j, \quad (13)$$

where B_{r_j} stands for the number of antenna-beams at relay j , $\forall j \in \{1, \dots, |\mathcal{R}|\}$; in the following we will assume $B_{r_j} = |\mathcal{S}|$. Thus the corresponding formulation for maximizing overall qualities of received HD video streams from sources to a destination is as follows:

$$\max : \sum_{i=1}^{|\mathcal{S}|} f_q \left(\sum_{j=1}^{|\mathcal{R}|} \frac{1}{2} a_{s_i \rightarrow r_j}^{\text{SRC}} x_{s_i \rightarrow r_j}^{\text{SRC}} \right) \quad (14)$$

subject to (6), (8), (9), (10), (11), (12), and (13).

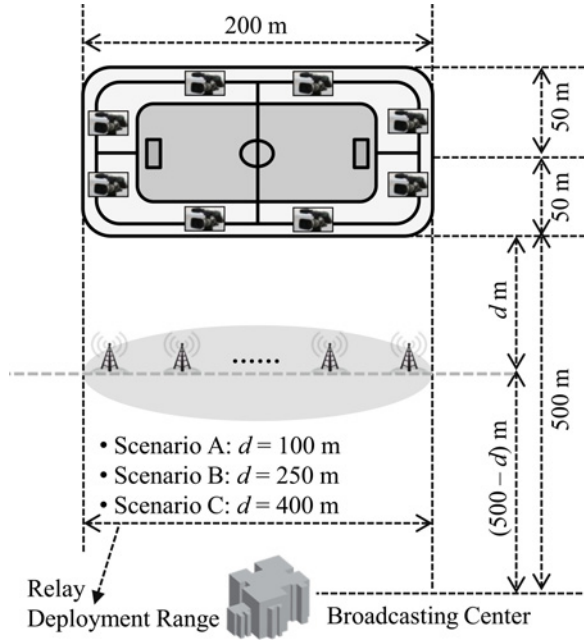


Fig. 5. Performance Evaluation Simulation Setup: Wireless HD video cameras are uniformly distributed on top of the stadium. There is one broadcasting center at bottom. Between wireless video cameras on top of stadium and broadcasting center, relays are uniformly and linearly deployed. To vary simulation setting, the deployment of relays has three different types: the relays are distributed near cameras (Scenario A), in the middle of cameras (on top of stadium) and broadcasting center (Scenario B), and near broadcasting center (Scenario C).

C. Multiple-Beam Antennas at Source and Relays

When the sources have multiple-beam antennas, the constraint (8) is updated to allow multiple outgoing flows for all sources as follows:

$$\sum_{j=1}^{|\mathcal{R}|} x_{s_i \rightarrow r_j}^{\text{SRC}} \leq B_{s_i}, \forall i. \quad (15)$$

where B_{s_i} stands for the number of antenna-beams at source i , $\forall i \in \{1, \dots, |\mathcal{S}|\}$; in the following we will assume $B_{s_i} = |\mathcal{R}|$.

Summarizing, the mathematical formulation can be again written as follows:

$$\max : \sum_{i=1}^{|\mathcal{S}|} f_q \left(\sum_{j=1}^{|\mathcal{R}|} \frac{1}{2} a_{s_i \rightarrow r_j}^{\text{SRC}} x_{s_i \rightarrow r_j}^{\text{SRC}} \right) \quad (16)$$

subject to (6), (9), (10), (11), (12), (13), and (15).

D. Discussion

In some cases direct transmission from source to a broadcasting center can guarantee better video quality than transmission via relay. This can be incorporated in our framework by placing a virtual relay (denoted as $r_{(v,j)}$ in this subsection) at a location very close to the destination, and letting the capacity between the relay and a broadcasting center be infinity (i.e., $\mathcal{A}_{r_{(v,j)} \rightarrow D}^{\text{RDC}} = \infty$), while the achievable capacity between source and relay is $2 \cdot \mathcal{A}_{s_i \rightarrow r_{(v,j)}}^{\text{SRC}}$, where the factor 2 reflects the fact that there is no half-duplex penalty in direct transmission.

V. RE-FORMULATION: CONVEX FORM

The proposed three mathematical formulations can be non-convex mixed-integer nonlinear programs (MINLP) even though the quality function has a convex form (Fig. 4) as shown in following theorem.

Theorem 1: The three optimization formulations in Section IV can be a non-convex MINLP.

Proof: If there exists a quality function which has logarithmically and monotonically increasing property (Fig. 4) which can make our designed mathematical formulation be non-convex MINLP, then the corresponding formulation is non-convex. Then, the following equation is one example of a possible quality index function:

$$f_q(a) = \frac{1}{\log_{\beta}(a_{\max} + 1)} \log_{\beta}(a + 1) \quad (17)$$

β is a base ($1 < \beta$), a_{\max} is a desired data rate for uncompressed video transmission (1.5 Gbit/s in a standard mode), and a is a given data rate. This proof considers the scenario of one-source and one-relay, which is the simplest case. In this case the objective function becomes

$$f \left(a_{s_i \rightarrow r_j}^{\text{SRC}}, x_{s_i \rightarrow r_j}^{\text{SRC}} \right) \triangleq f_q \left(a_{s_i \rightarrow r_j}^{\text{SRC}} \right) x_{s_i \rightarrow r_j}^{\text{SRC}} \quad (18)$$

$$= \mathcal{K} \log_{\beta} \left(a_{s_i \rightarrow r_j}^{\text{SRC}} + 1 \right) x_{s_i \rightarrow r_j}^{\text{SRC}} \quad (19)$$

where $\mathcal{K} = \frac{1}{\log_{\beta}(a_{\max} + 1)}$ is a constant and $\forall i \in \{1, \dots, |\mathcal{S}|\}, \forall j \in \{1, \dots, |\mathcal{R}|\}$. To show that this given equation is non-convex, the second-order Hessian of this given real function should be non positive definite [26]. The Hessian $\nabla^2 f \left(a_{s_i \rightarrow r_j}^{\text{SRC}}, x_{s_i \rightarrow r_j}^{\text{SRC}} \right)$ is:

$$\begin{bmatrix} 0 & \frac{\mathcal{K}}{\ln \beta} \cdot \frac{1}{a_{s_i \rightarrow r_j}^{\text{SRC}} + 1} \\ \frac{\mathcal{K}}{\ln \beta} \cdot \frac{1}{a_{s_i \rightarrow r_j}^{\text{SRC}} + 1} & -x_{s_i \rightarrow r_j}^{\text{SRC}} \cdot \frac{\mathcal{K}}{\ln \beta} \cdot \left(\frac{1}{a_{s_i \rightarrow r_j}^{\text{SRC}} + 1} \right)^2 \end{bmatrix} \quad (20)$$

and then the corresponding two eigenvalues are

$$\frac{1}{2} \mathcal{M} \pm \frac{1}{2} \left\{ \mathcal{M}^2 + 4 \left(\frac{\mathcal{K}}{\ln \beta} \cdot \frac{1}{a_{s_i \rightarrow r_j}^{\text{SRC}} + 1} \right)^2 \right\}^{0.5} \quad (21)$$

where $\mathcal{M} = -x_{s_i \rightarrow r_j}^{\text{SRC}} \cdot \frac{\mathcal{K}}{\ln \beta} \cdot \left(\frac{1}{a_{s_i \rightarrow r_j}^{\text{SRC}} + 1} \right)^2$, $0 \leq a_{s_i \rightarrow r_j}^{\text{SRC}} \leq 1.5$, and $0 \leq x_{s_i \rightarrow r_j}^{\text{SRC}} \leq 1$. These values are not all positive, which shows that the Hessian is not positive definite, which proves that the optimization function is non-convex. ■

For non-convex MINLP, heuristic searches can find approximate solutions but cannot guarantee optimality. Among well-known approximation algorithms, branch-and-refine based algorithms show relatively better performance for non-convex MINLP problems [27]. The detailed procedure of the branch-and-refine based algorithms is as follows: First, the integer terms are relaxed (relaxation), i.e., $x_{s_i \rightarrow r_j}^{\text{SRC}} \in \{0, 1\}$ is converted to $0 \leq x_{s_i \rightarrow r_j}^{\text{SRC}} \leq 1$. After that, the special ordered sets (SOS) approximation is used for a linear approximation. This segments the multi-dimensional space of the given objective

TABLE II

EXPECTATION OF ACHIEVED AGGREGATED VIDEO QUALITY FOR SINGLE-BEAM ANTENNAS AT SOURCES AND RELAYS CASE (VALUES: THE OBJECTIVE FUNCTION RESULTS WITH OPTIMAL SOLUTIONS)

$ \mathcal{S} $	$ \mathcal{R} $	Scenario	VQM	SRM	JRSR
5	10	A	4.15	3.33	3.33
5	10	B	4.92	4.17	4.17
5	10	C	4.41	3.63	3.63
5	10	Random	4.43	3.65	3.65
10	5	A	4.15	3.35	3.35
10	5	B	4.92	4.18	4.18
10	5	C	4.41	3.65	3.65
10	5	Random	4.43	3.67	3.67
10	10	A	8.74	5.48	5.48
10	10	B	9.54	6.34	6.34
10	10	C	8.95	5.79	5.79
10	10	Random	9.17	5.20	5.20
10	15	A	8.78	5.63	5.63
10	15	B	9.79	6.46	6.46
10	15	C	9.18	5.93	5.93
10	15	Random	9.19	5.85	5.85
15	10	A	9.11	6.48	6.48
15	10	B	9.89	7.38	7.38
15	10	C	9.37	6.84	6.84
15	10	Random	9.39	6.85	6.85

TABLE III

EXPECTATION OF ACHIEVED AGGREGATED VIDEOQUALITY FOR SINGLE-BEAM ANTENNAS AT SOURCES AND MULTIPLE-BEAM ANTENNAS AT RELAYS CASE (VALUES: THE OBJECTIVE FUNCTION RESULTS WITH OPTIMAL SOLUTIONS)

$ \mathcal{S} $	$ \mathcal{R} $	Scenario	VQM	SRM	JRSR
5	10	A	4.15	3.85	3.33
5	10	B	4.92	4.60	4.17
5	10	C	4.65	4.35	3.63
5	10	Random	4.57	4.27	3.65
10	5	A	4.16	3.86	3.35
10	5	B	4.95	4.61	4.18
10	5	C	4.66	4.36	3.65
10	5	Random	4.57	4.28	3.67
10	10	A	8.81	8.46	5.48
10	10	B	9.81	9.46	6.34
10	10	C	9.31	8.96	5.79
10	10	Random	9.29	8.96	5.20
10	15	A	8.86	8.55	5.63
10	15	B	9.86	9.55	6.46
10	15	C	9.36	9.05	5.93
10	15	Random	9.36	9.04	5.85
15	10	A	13.41	11.70	6.48
15	10	B	14.88	13.20	7.38
15	10	C	14.38	12.71	6.84
15	10	Random	14.22	12.53	6.85

function into multiple small triangular regions, each of which is plane; in other words, the triangle regions approximate the multi-dimensional surface of the objective function. For every single triangle region, optimum solutions can be obtained by running a simplex based algorithm. Then, we run the branch-and-bound algorithm to find integer solutions for $x_{s_i \rightarrow r_j}^{\text{SRC}}$ for each single triangle region. Thus finally the optimum value is selected among the solutions on the triangles. However, the branch-and-refine algorithm cannot guarantee the optimum solutions in a non-convex MINLP. First of all, if the segmentation into plane triangle regions is rough, then the approximated planes are not precise enough to get the optimum solutions. If the segmentation into plane triangle regions is too fine, the runtime becomes excessive, since the simplex algorithm should be operated for every single triangular region. In conclusion, using branch-and-refine based algorithm provides an approximation but cannot guarantee the optimum solutions and, moreover, this algorithm cannot find bounds on the approximation errors. We thus introduce the following Theorem, with which our non-convex MINLP can be re-formulated as a convex program.

Theorem 2: For the given non-convex MINLP formulation in Section IV, introducing

$$a_{s_i \rightarrow r_j}^{\text{SRC}} \leq \mathcal{A}_{s_i \rightarrow r_j}^{\text{SRC}} \cdot x_{s_i \rightarrow r_j}^{\text{SRC}}, \forall i, \forall j \quad (22)$$

instead of (10) makes the formulation convex.

Proof: For the non-convex MINLP formulation in Section IV, $x_{s_i \rightarrow r_j}^{\text{SRC}} = 0$ means the link is disconnected. Thus

the corresponding rate becomes 0 and (22) leads to the same result when $x_{s_i \rightarrow r_j}^{\text{SRC}} = 0$, i.e.,

$$a_{s_i \rightarrow r_j}^{\text{SRC}} \leq \mathcal{A}_{s_i \rightarrow r_j}^{\text{SRC}} \cdot 0, \forall i, \forall j, \quad (23)$$

thus,

$$a_{s_i \rightarrow r_j}^{\text{SRC}} \leq 0, \forall i, \forall j. \quad (24)$$

and then $a_{s_i \rightarrow r_j}^{\text{SRC}}$ is equal to 0 because $a_{s_i \rightarrow r_j}^{\text{SRC}}$ is non-negative. Otherwise, if $x_{s_i \rightarrow r_j}^{\text{SRC}} = 1$, then this term is equivalent to (10). Therefore, in turn, (5), (14), (16) are also updated as

$$\max : \sum_{i=1}^{|\mathcal{S}|} f_q \left(\sum_{j=1}^{|\mathcal{R}|} \frac{1}{2} a_{s_i \rightarrow r_j}^{\text{SRC}} \right), \quad (25)$$

(6) is updated as follows

$$\sum_{i=1}^{|\mathcal{S}|} a_{s_i \rightarrow r_j}^{\text{SRC}} \leq \mathcal{A}_{r_j \rightarrow D}^{\text{RDC}}, \forall j, \quad (26)$$

and (9) is also updated as follows

$$a_{s_i} \leq \sum_{j=1}^{|\mathcal{R}|} a_{s_i \rightarrow r_j}^{\text{SRC}}, \forall i. \quad (27)$$

Then there are no non-convex terms in the proposed programs. ■

Summarizing, the optimization problem can be reformulated as follows. For the single-beam antennas at sources and relays

$$\max : \sum_{i=1}^{|\mathcal{S}|} f_q \left(\sum_{j=1}^{|\mathcal{R}|} \frac{1}{2} a_{s_i \rightarrow r_j}^{\text{SRC}} \right) \quad (28)$$

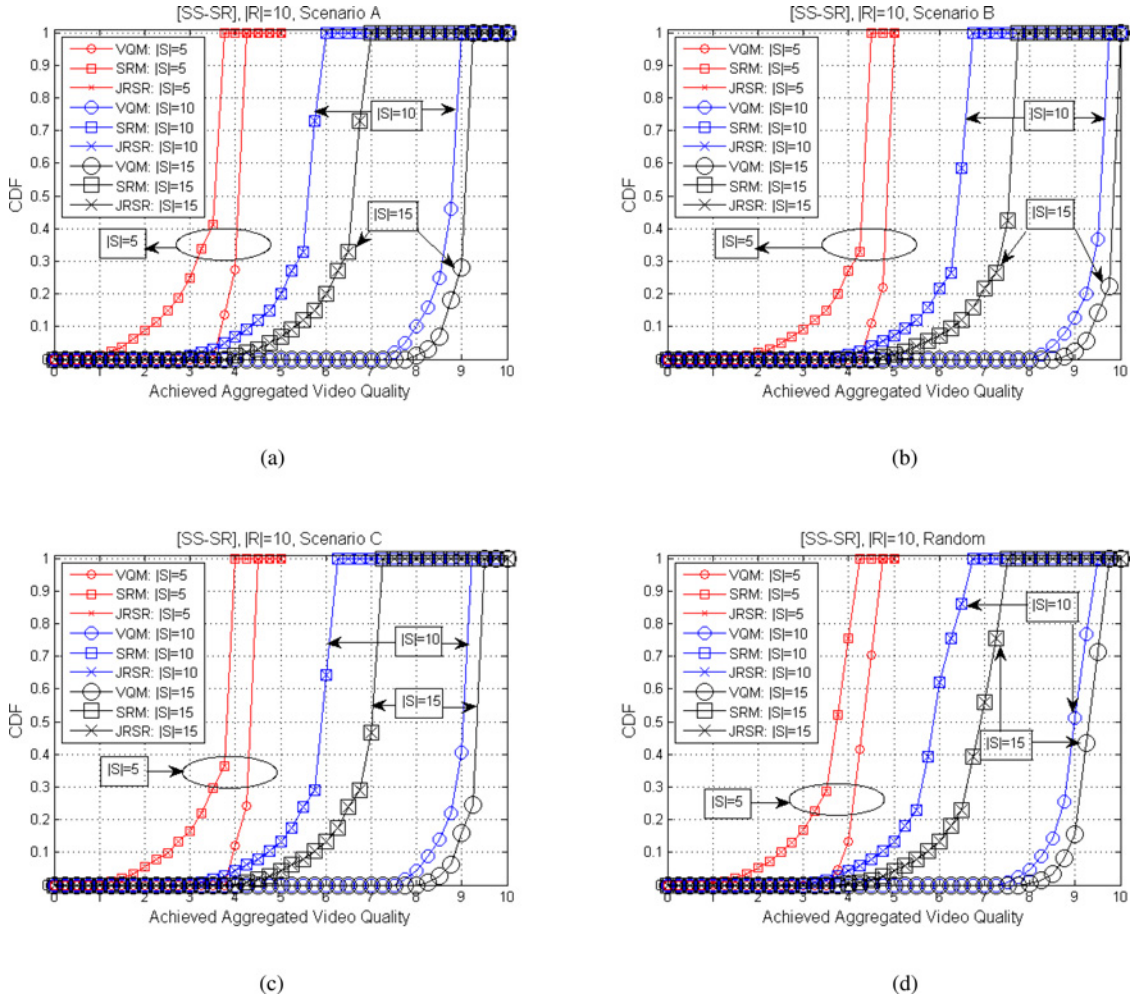


Fig. 6. Simulation Result for Single-Beam Antennas at Sources and Relays: Various Number of Sources ($|\mathcal{S}| = 5, 10, 15$) and Fixed Number of Relays ($|\mathcal{R}| = 10$), (a) Scenario A, (b) Scenario B, (c) Scenario C, (d) Random.

subject to

$$\sum_{i=1}^{|\mathcal{S}|} a_{s_i \rightarrow r_j}^{\text{SRC}} \leq \mathcal{A}_{r_j \rightarrow D}^{\text{RDC}}, \forall j, \quad (29)$$

$$\sum_{i=1}^{|\mathcal{S}|} x_{s_i \rightarrow r_j}^{\text{SRC}} \leq 1, \forall j, \quad (30)$$

$$\sum_{j=1}^{|\mathcal{R}|} x_{s_i \rightarrow r_j}^{\text{SRC}} \leq 1, \forall i, \quad (31)$$

$$a_{s_i} \leq \sum_{j=1}^{|\mathcal{R}|} a_{s_i \rightarrow r_j}^{\text{SRC}}, \forall i, \quad (32)$$

$$a_{s_i \rightarrow r_j}^{\text{SRC}} \leq \mathcal{A}_{s_i \rightarrow r_j}^{\text{SRC}} \cdot x_{s_i \rightarrow r_j}^{\text{SRC}}, \forall i, \forall j, \quad (33)$$

$$x_{s_i \rightarrow r_j}^{\text{SRC}} \in \{0, 1\}, \forall i, \forall j, \quad (34)$$

$$x_{r_j \rightarrow D}^{\text{RDC}} = 1, \forall j, \quad (35)$$

where $\forall i \in \{1, \dots, |\mathcal{S}|\}, \forall j \in \{1, \dots, |\mathcal{R}|\}$. In addition, for the single-beam antennas at sources and multiple-beam antennas at relays case, the objective function is equivalent to (28) and the corresponding constraints are (29), (31), (32), (33), (34), (35), and (13) where $\forall i \in \{1, \dots, |\mathcal{S}|\}, \forall j \in \{1, \dots, |\mathcal{R}|\}$ and finally for the multiple-beam antennas at source and relays case, the objective function is equivalent to (28) and the corresponding constraints are (29), (32), (33), (34), (35), (13), and (15) where $\forall i \in \{1, \dots, |\mathcal{S}|\}, \forall j \in \{1, \dots, |\mathcal{R}|\}$.

With these given convex programs, the given integer constraints, i.e., $x_{s_i \rightarrow r_j}^{\text{SRC}} \in \{0, 1\}$ are relaxed as $0 \leq x_{s_i \rightarrow r_j}^{\text{SRC}} \leq 1$, $\forall i \in \{1, \dots, |\mathcal{S}|\}, \forall j \in \{1, \dots, |\mathcal{R}|\}$. Then the convex programs are solved using CVX which is the most popular matlab-based software for solving convex optimization problems [28].

VI. PERFORMANCE EVALUATION

To verify the superior performance of our proposed scheme, i.e., a joint HD video coding rate decision and relay selection/routing scheme under the consideration of overall video quality maximization (named VQM), we compare it with the following two schemes:

- 1) The joint HD video coding rate decision and relay selection/routing scheme under the consideration of *sum rate maximization*. In this case, the proposed objective function, i.e., (28), should be updated as follows:

$$\max : \sum_{i=1}^{|\mathcal{S}|} \left(\sum_{j=1}^{|\mathcal{R}|} \frac{1}{2} a_{s_i \rightarrow r_j}^{\text{SRC}} \right) \quad (36)$$

due to the fact that the quality function (Fig. 4) is no longer considered. Note that the half-duplex constraint is still existing. This method is named as SRM, i.e., sum rate maximization.

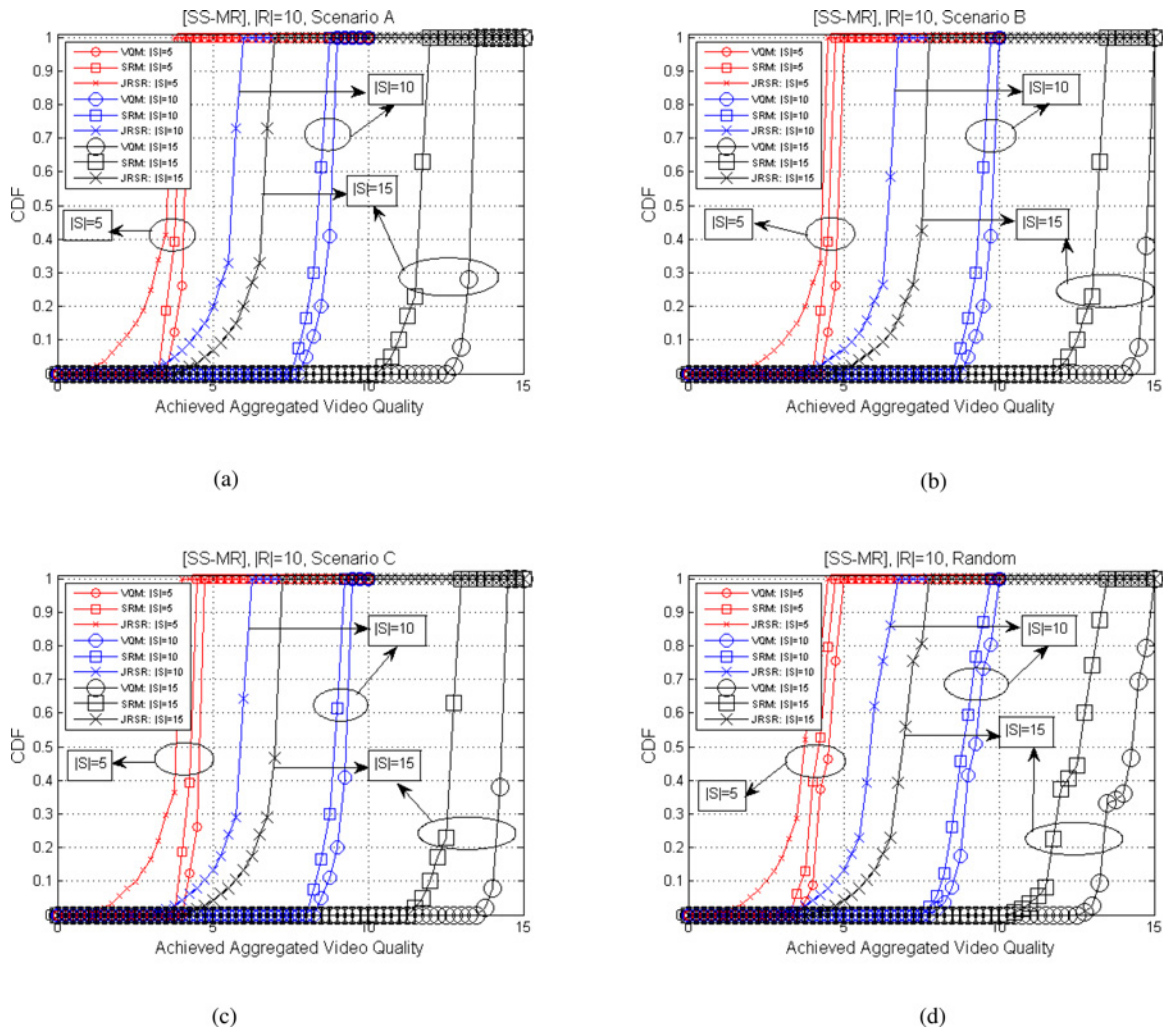


Fig. 7. Simulation Result for Single-Beam Antennas at Sources and Multiple-Beam Antennas at Relays: Various Number of Sources ($|S| = 5, 10, 15$) and Fixed Number of Relays ($|\mathcal{R}| = 10$), (a) Scenario A, (b) Scenario B, (c) Scenario C, (d) Random.

2) The scheme proposed in [14], which is an efficient algorithm that considers joint relay selection/routing (called JRSR) and rate allocation at the same time. In order to enable fair comparisons, we adapt the scheme to our outdoor-stadium architecture (one-tier relay) and allow only decode-and-forward relaying. Lastly, Ref. [14] has the same number of sources and destinations; however, to unify the setup for performance comparison, all the given destinations are located at the same location and operate as a single destination with multiple antenna elements.

With these given three schemes, i.e., VQM, SRM, JRSR, overall delivered video quality values are simulated in the reference models shown in Fig. 5. The sources (HD cameras) are uniformly distributed on top of the stadium. Between stadium and broadcasting center, multiple relays are uniformly deployed along a line. To vary the simulation scenarios, we consider this line to be near the sources (Scenario A), in the middle between sources and broadcast center (Scenario B), and near the broadcast center (Scenario C). Lastly, we also consider a scenario where the relay positions are uniformly

randomly distributed. In Scenario A, there is a higher probability that the relay-to-destination link might be the bottleneck, while Scenario C obviously has the source-relay link as its bottleneck.

In addition, for the simulation studies with multiple antenna-beams at sources or relays, the number of beams at relays and the number of beams at sources are set as $|S|$ and $|\mathcal{R}|$, respectively.

As our performance measure we consider the cumulative probability distribution of the aggregate video quality. We will show results for a fixed number of relays ($|\mathcal{R}| = 10$) and various number of sources ($|S| = 5, 10, 15$) at first (Sec. VI-A). The cdf is obtained as follows: we consider multiple realizations of the deployment of sources and relays (for a fixed scenario and number of relays, but random relay location according to the location pdf of a given scenario). For each such realization, we optimize coding rates and relay selection; thus each run gives us one realization of the aggregate video quality. We finally plot the cdf of this quality. For the simulation of VQM, the lower bounds of each flow are set as 0.75, i.e., all \underline{a}_i where $\forall i \in \{1, \dots, |S|\}$ are all set to

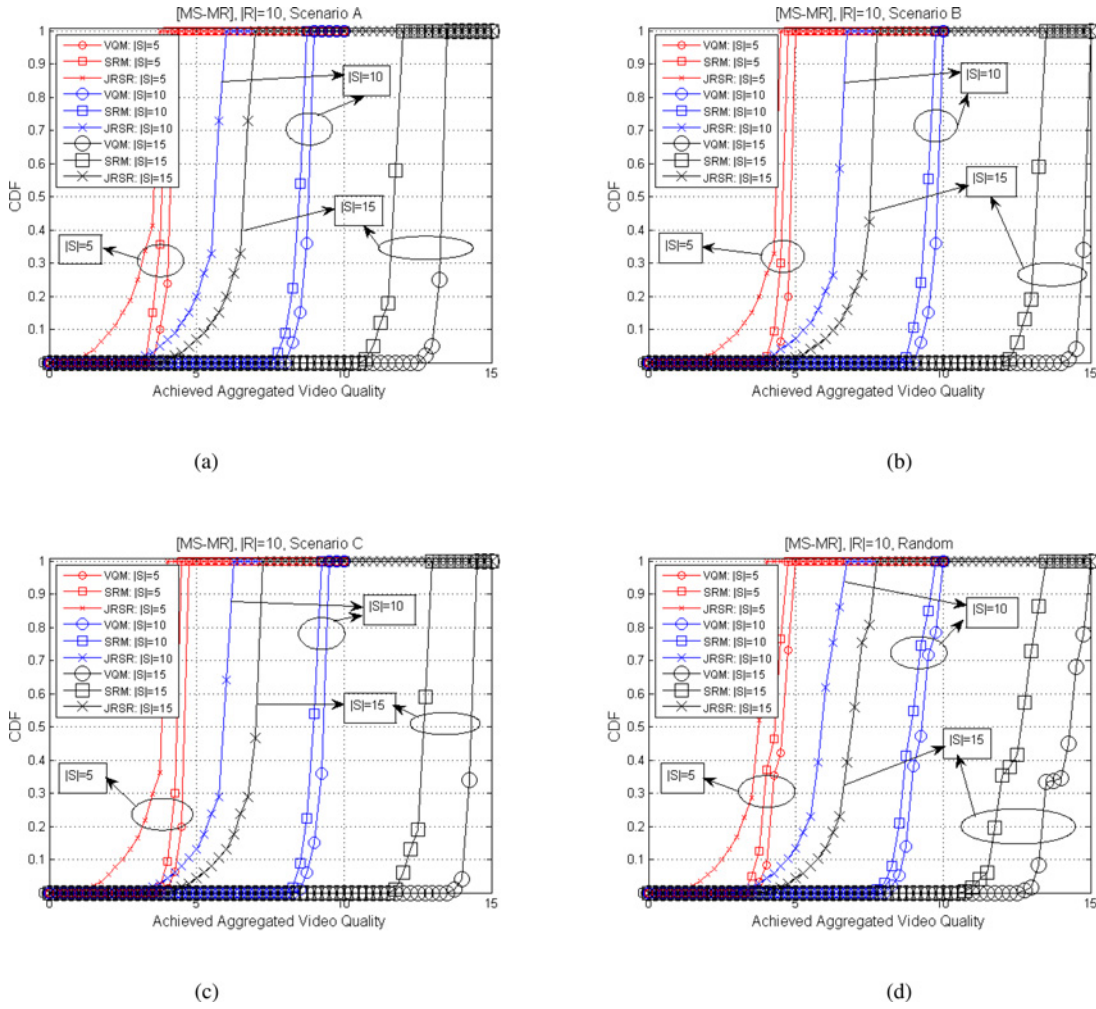


Fig. 8. Simulation Result for Multiple-Beam Antennas at Sources and Relays: Various Number of Sources ($|\mathcal{S}| = 5, 10, 15$) and Fixed Number of Relays ($|\mathcal{R}| = 10$), (a) Scenario A, (b) Scenario B, (c) Scenario C, (d) Random.

0.75 (Unit: Gbit/s) in a standard mode (i.e., 50% of 1.5 Gbit/s). Later, Section VI-C shows the performance behavior if various lower bound settings are observed.

A. CDF of Aggregate Video Quality – Fixed Number of Relays and Various Number of Sources

1) *Single-Beam Antennas at Sources and Relays*: Fig. 6 presents the cases that the number of sources is smaller, equal, or larger than the number of relays (i.e., $|\mathcal{S}| = 5, 10, 15$, and $|\mathcal{R}| = 10$). We see that SRM and JRSR show the same performance because they are equivalent for the given constraints of single-beam antennas at sources and relays. For the case of 5 sources, we also see that with the proposed VQM, the aggregate video quality is within 5% of its maximum for 83% of simulation runs in Scenario A, 98% of simulation runs in Scenario B, 88% of simulation runs in Scenario C and 89% of random deployment. Note that the given number of sources is 5, thus, the maximum achievable video quality is 5 due to the fact that the maximum video quality index in each flow is normalized as 1 (refer to Fig. 4). We also find that deployment scenario Scenario B can obtain more quality than the others deployment scenarios since it best balances capacity constraints on the source-relay and relay-destination

links. The mean achieved aggregate video qualities are also given in Table II. For the case of 10 or 15 sources, the maximum achievable aggregated video quality is 10 because the given number of relays is 10 which takes a role of threshold of the delivered quality.

2) *Single-Beam Antennas at Sources and Multiple-Beam Antennas at Relays*: Fig. 7 and Table III present data similar to Fig. 6 and Table II, but now with multiple-beam antennas at the relays, so that the relays can aggregate and combine video streams from different sources. In this case, there exists a performance difference between SRM and JRSR. The latter, by design, does not allow the exploitation of the multiple-beam antennas at relays, and thus shows worse performance. As a matter of fact, it has the same performance as with single-beam antennas at sources and relays case if the network configuration is equivalent. This fact will even hold in the case of multiple-beam antennas at sources and relays. We furthermore see that again SRM shows lower performance than VQM due to the fact that SRM aims for maximization of sum data rates, while VQM aims to maximize the overall delivered video quality. We also see that for the case that the number of relays is sufficient (larger than or equal to the number of sources), the achieved video quality is not

TABLE IV

EXPECTATION OF ACHIEVED AGGREGATED VIDEO QUALITY FOR MULTIPLE-BEAM ANTENNAS AT SOURCES AND RELAYS CASE (VALUES: THE OBJECTIVE FUNCTION RESULTS WITH OPTIMAL SOLUTIONS)

$ \mathcal{S} $	$ \mathcal{R} $	Scenario	VQM	SRM	JRSR
5	10	A	4.16	3.8734	3.3313
5	10	B	4.93	4.6469	4.1650
5	10	C	4.68	4.3969	3.6315
5	10	Random	4.59	4.3057	3.6534
10	5	A	4.16	3.87	3.35
10	5	B	4.95	4.62	4.18
10	5	C	4.66	4.37	3.65
10	5	Random	4.58	4.29	3.67
10	10	A	8.81	8.45	5.48
10	10	B	9.82	9.45	6.34
10	10	C	9.31	8.96	5.79
10	10	Random	9.31	8.85	5.20
10	15	A	8.88	8.57	5.63
10	15	B	9.87	9.56	6.46
10	15	C	9.38	9.07	5.93
10	15	Random	9.38	9.07	5.85
15	10	A	13.42	11.77	6.48
15	10	B	14.90	13.25	7.38
15	10	C	14.40	12.76	6.84
15	10	Random	14.24	12.59	6.85

fundamentally different from the case with single-beam antennas at the relays. However, this changes when the number of relays is not sufficient (i.e., $|\mathcal{S}| = 15$, $|\mathcal{R}| = 10$). We can now achieve aggregate video quality larger than 10 as some streams can be compressed with little video quality loss and forwarded by the same relay. Nonideal performance is mainly caused by the capacity limitations of the relay-destination links. These limitations have more impact on scenarios A and B than in Scenario C.

3) *Multiple-Beam Antennas at Sources and Relays*: For multiple-beam antennas at both sources and relays, VQM and SRM have better performance than the case of single-beam antennas at sources, while JRSR has the same performance as in the case of single-beam antennas as described above. We also note that in this case, the optimization for SRM can be solved by a maximum flow formulation as shown in Appendix A. With the benefit of multiple-beam antennas, SRM and VQM have better performance than the other two cases as shown in Fig. 8 and Table IV; however, the performance gain is minor. As in the single-beam case at the source, the achieved aggregated video quality is limited by the capacity between relays and a destination.

B. Expectation of Achieved Aggregated Video Quality

This section evaluates the performance of VQM in terms of expected achieved aggregated video quality. We varied the numbers of sources and relays from 0 to 15 with 4 steps, i.e., 0, 5, 10, 15. Then, the expectation of achieved aggregated video quality is obtained for the given numbers of

TABLE V

EXPECTATION OF ACHIEVED AGGREGATED VIDEO QUALITY FOR SINGLE-BEAM ANTENNAS AT SOURCES AND RELAYS CASE (SEC. VI-B)

	$ \mathcal{S} = 5$	$ \mathcal{S} = 10$	$ \mathcal{S} = 15$
$ \mathcal{R} = 5$	4.23	4.50	4.60
$ \mathcal{R} = 10$	4.49	9.08	9.46
$ \mathcal{R} = 15$	4.59	9.25	12.14

TABLE VI

EXPECTATION OF ACHIEVED AGGREGATED VIDEO QUALITY FOR SINGLE-BEAM ANTENNAS AT SOURCES AND MULTIPLE-BEAM ANTENNAS AT RELAYS CASE (SEC. VI-B)

	$ \mathcal{S} = 5$	$ \mathcal{S} = 10$	$ \mathcal{S} = 15$
$ \mathcal{R} = 5$	4.43	4.59	4.69
$ \mathcal{R} = 10$	4.58	9.31	14.22
$ \mathcal{R} = 15$	4.68	9.36	14.91

TABLE VII

EXPECTATION OF ACHIEVED AGGREGATED VIDEO QUALITY FOR MULTIPLE-BEAM ANTENNAS AT SOURCES AND RELAYS CASE (SEC. VI-B)

	$ \mathcal{S} = 5$	$ \mathcal{S} = 10$	$ \mathcal{S} = 15$
$ \mathcal{R} = 5$	4.45	4.59	4.69
$ \mathcal{R} = 10$	4.59	9.31	14.24
$ \mathcal{R} = 15$	4.69	9.38	14.96

sources and relays. The result of the single-beam antennas at sources and relays case is presented in Fig. 9(a) and Table V. Similarly the results of the other two cases are presented in Fig. 9(b)/Fig. 9(c) and Table VI/Table VII.

As shown in these three figures and tables, if we allow more beams to relays or sources, then we can obtain higher video quality. In addition, if we have more relays or sources, then we can similarly increase aggregate video quality.

C. Impact of Lower Bound Setting

In the previous simulations, the lower bounds for the data rate per data stream (corresponding to the desired lower bound on the video quality) are set as 0.75 Gbit/s. In this section, we vary now this lower bound values from 0 Gbit/s (i.e., there is no lower bound) up to 1.5 Gbit/s (i.e., we allow only uncompressed HD video transmission) in steps of 0.1 Gbit/s. As a performance quality measure we define “stream outage”, i.e., the probability that at least one stream does not have the minimum required quality. Obviously, this outage has to increase (and thus its complement, the probability of successful transmission, has to decrease) as the minimum video quality increases. We furthermore anticipate that VQM will be better able to handle the increased requirements, as it is more flexible.

This evaluation is performed for the case of single-beam antennas at the sources and multiple-beam antennas at relays when $|\mathcal{S}| = 10$, $|\mathcal{R}| = 15$ in Fig. 10.

As shown in Fig. 10, the case of relay deployment with Scenario C suffers significantly from the higher required

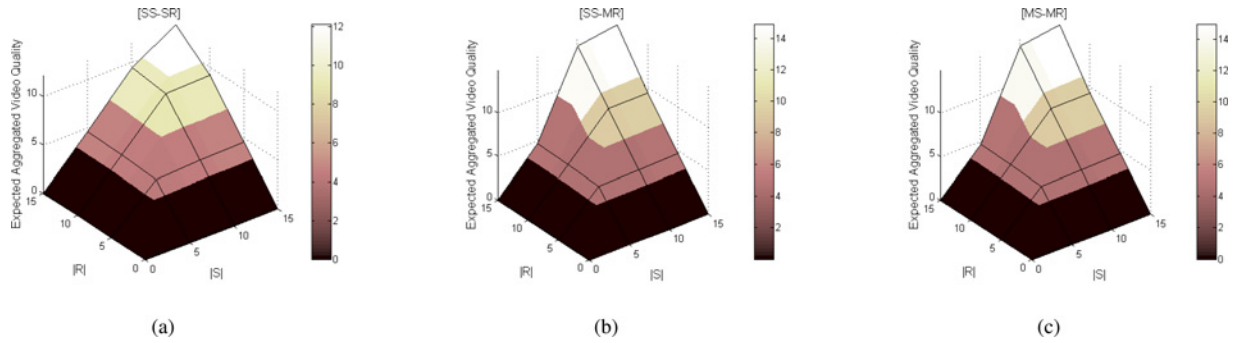


Fig. 9. Simulation Result for Expectation of Achieved Aggregated Video Quality, (a) Scenario A, (b) Scenario B, (c) Scenario C.

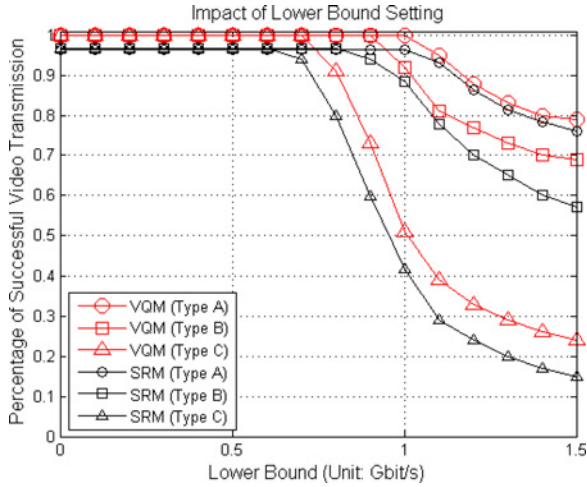


Fig. 10. Simulation Result for Various Lower Bound Setting: Single-Beam Antennas at Sources and Multiple-Beam Antennas at Relays, $|S| = 10$, $|\mathcal{R}| = 15$.

per-stream quality. With Scenario C relay deployment, the data rates between sources and relays are lower than in the other cases. Thus, when we set the lower bound quite high, all flows are disconnected. Thus, it achieves the lowest performance. On the other hand, in Scenario A relay deployment, all flows between sources and relays have enough capacity to support uncompressed video transmission, thus, a higher setting for minimum quality does not have such a strong impact. In addition, Fig. 10 shows that VQM has better performance than SRM for all possible three types of relay deployment. For more details, the average normalized video quality for VQM is 0.9531, 0.9138, 0.7288 for Scenario A, B, C, respectively. SRM cannot achieve maximum aggregated video quality due to the fact that it maximizes the overall data rates instead of overall delivered video qualities.

VII. CONCLUDING REMARKS

This paper addresses a joint scalable coding and routing scheme for a 60 GHz millimeter-wave HD video streaming in an outdoor sports stadium broadcasting system. In the system, there are multiple wireless HD video cameras distributed throughout the stadium. To transmit the HD video data from the cameras over the wireless channels in a real-time manner,

60 GHz wireless links are used because they can exploit multi-Gbit/s wireless data transmission. However, according to the high path loss of 60 GHz links, relays are used to extend communication coverage. We presented an algorithm for finding the combination of wireless link pairs between wireless HD video cameras and relays that can maximize the overall or per-flow video qualities of delivered HD video streams to one single broadcasting center. This paper considers three kinds of cases, i.e., single-beam antennas at sources and relays, single-beam antennas at sources and multiple-beam antennas at relays, and finally, multiple-beam antennas at sources and relays. For each cases, the given problem is initially formulated as non-convex MINLP and it is re-formulated as convex program, which allows optimum solutions.

We demonstrated that our algorithm outperforms algorithms based on sum-rate maximization and other well-known methods in the literature, for a variety of relay deployment scenarios, number of sources, and number of relays.

APPENDIX A
MAXIMUM FLOW FORMULATION

In the proposed scheme, sum quality maximization is considered because our aim is the maximization of achieved aggregated video quality. However, if we consider sum *rate* maximization instead of sum *quality* maximization with multiple-beam antennas at sources and relays, our problem is equivalent to the maximum network flow problem and thus can be solved by the Edmonds-Karp algorithm. In our reference network model (refer to Fig. 3), s_v should be added as a virtual source to start the flows, i.e., it is connected to all sources, i.e., $s_i, \forall i$. Then, all individual flows from s_v to $s_i, \forall i$, are limited by \mathcal{A}_{\max} , thus the wireless link capacities (i.e., maximum achievable rates) between s_v and $s_i, \forall i$ are set to be all \mathcal{A}_{\max} . The link capacities between relays $r_j, \forall j$ and destination D are defined as the maximum achievable rates between the relays and destination, i.e., $\mathcal{A}_{r_j \rightarrow D}^{\text{RDC}}, \forall j$ and these values are upper bounds for the corresponding links. The links between all sources $s_i, \forall i$ and all relays $r_j, \forall j$ are limited by the maximum achievable rates, i.e., $\mathcal{A}_{s_i \rightarrow r_j}^{\text{SRC}}, \forall i, \forall j$ and these values are upper bounds for the corresponding wireless links. With these configurations, the Edmonds-Karp algorithm finds the maximum achievable rate flows from all sources $s_i, \forall i$ towards one destination D via relays $r_j, \forall j$.

REFERENCES

- [1] P. Smulders, "Exploiting the 60 GHz band for local wireless multimedia access: Prospects and future directions," *IEEE Commun. Mag.*, vol. 40, no. 1, pp. 140–147, Jan. 2002.
- [2] H. Singh, J. Oh, C. Kweon, X. Qin, H.-R. Shao, and C. Ngo, "A 60 GHz wireless network for enabling uncompressed video communication," *IEEE Commun. Mag.*, vol. 12, no. 46, pp. 71–78, Dec. 2008.
- [3] WirelessHD [Online]. Available: <http://wirelesshd.org>
- [4] Wireless Gbit Alliance (WiGig) [Online]. Available: <http://wirelessgbitalliance.org>
- [5] *IEEE 802.15.3c Millimeter-Wave-Based Alternative Physical Layer Extension*. (2009, Oct.) [Online]. Available: <http://www.ieee802.org/15/pub/TG3c.html>
- [6] IEEE 802.11ad VHT Specification Ver. 1.0, Dec. 2012.
- [7] H. Su and X. Zhang, "Joint link scheduling and routing for directional-antenna based 60 GHz wireless mesh networks," in *Proc. IEEE GLOBECOM*, Dec. 2009, pp. 6192–6197.
- [8] M. M. Akbar, M. S. Rahman, M. Kaykobad, E. G. Manning, and G. C. Shoja, "Solving the multidimensional multiple-choice knapsack problem by constructing convex hulls," *Comput. Oper. Res.*, vol. 33, no. 5, pp. 1259–1273, May 2006.
- [9] D. Giustiniano, V. Vukadinovic, and S. Mangold, "Wireless networking for automated live video broadcasting: System architecture and research challenges," in *Proc. IEEE WoWMoM*, Jun. 2011, pp. 1–9.
- [10] M.-H. Lu, P. Steenkiste, and T. Chen, "Time-aware opportunistic relay for video streaming over WLANs," in *Proc. IEEE ICME*, Jul. 2007, pp. 1782–1785.
- [11] S. Mao, X. Cheng, Y. T. Hou, H. D. Sherali, and J. Reed, "On joint routing and server selection for MD video streaming in ad hoc networks," *IEEE Trans. Wireless Commun.*, vol. 6, no. 1, pp. 338–347, Jan. 2007.
- [12] W. Wei and A. Zakhori, "Interference aware multipath selection for video streaming in wireless ad hoc networks," *IEEE Trans. Circuits Syst. Video Technol.*, vol. 19, no. 2, pp. 165–178, Feb. 2009.
- [13] S. Murthy, P. Hegde, V. Parameswaran, B. Li, and A. Sen, "Improved path selection algorithms for multipath video streaming in wireless ad hoc networks," in *Proc. IEEE MILCOM*, Oct. 2007.
- [14] S. Sharma, Y. Shi, Y. T. Hou, H. D. Sherali, S. Kompella, and S. F. Midkiff, "Joint flow routing and relay node assignment in cooperative multi-hop networks," *IEEE J. Select. Areas Commun.*, vol. 30, no. 2, pp. 254–262, Feb. 2012.
- [15] S. Singh, R. Mudumbai, and U. Madhow, "Interference analysis for highly directional 60-GHz mesh networks: The case for rethinking medium access control," *IEEE/ACM Trans. Netw.*, vol. 19, no. 5, pp. 1513–1527, Oct. 2011.
- [16] J. Kim, Y. Tian, A. F. Molisch, and S. Mangold, "Joint optimization of HD video coding rates and unicast flow control for IEEE 802.11ad relaying," in *Proc. IEEE PIMRC*, Sep. 2011, pp. 1109–1113.
- [17] A. F. Molisch, *Wireless Communications*, 2nd ed. New York, NY, USA: Wiley-IEEE, 2011.
- [18] Comotech Corporation [Online]. Available: <http://www.comotech.com/en/index.html>
- [19] Millitech [Online]. Available: <http://www.millitech.com/>
- [20] H. Zhai, X. Chen, and Y. Fang, "Improving transport layer performance in multihop ad hoc networks by exploiting MAC layer information," *IEEE Trans. Wireless Commun.*, vol. 6, no. 5, pp. 1692–1701, May 2007.
- [21] M.-C. Hwang, J.-H. Kim, D. T. Duong, and S.-J. Ko, "Hybrid temporal error concealment methods for block-based compressed video transmission," *IEEE Trans. Broadcast.*, vol. 54, no. 2, pp. 198–197, Jun. 2008.
- [22] L. Zhou, B. Geller, B. Zheng, A. Wei, and J. Cui, "System scheduling for multi-description video streaming over wireless multi-hop networks," *IEEE Trans. Broadcast.*, vol. 55, no. 4, pp. 731–741, Dec. 2009.
- [23] H. L. Cycon, V. George, G. Hege, D. Marpe, M. Palkow, T. C. Schmidt, and M. Wahlisch, "Adaptive temporal scalability of H.264-compliant video conferencing in heterogeneous mobile environments," in *Proc. IEEE GLOBECOM*, Dec. 2010, pp. 1–5.
- [24] M.-P. Kao and T. Q. Nguyen, "Rate-distortion optimized bitstream extractor for motion scalability in wavelet-based scalable video coding," *IEEE Trans. Image Process.*, vol. 19, no. 5, pp. 1214–1223, May 2010.
- [25] C.-Y. Tsai and H.-M. Hang, "Rate-distortion model for motion prediction efficiency in scalable wavelet video coding," in *Proc. IEEE Packet Video Workshop*, May 2009, pp. 1–9.
- [26] S. Boyd and L. Vandenberghe, *Convex Optimization*. Cambridge, U.K.: Cambridge Univ. Press, 2004.
- [27] S. Leyffer, A. Sartenauer, and E. Wanufelle, "Branch-and-refine for mixed-integer nonconvex global optimization," *Math. Comput. Sci.* Division, Argonne Natl. Lab., ANL.MCS-Argonne, IL, USA, Tech. Rep., 2008.
- [28] M. Grant and S. Boyd, *CVX: Matlab Software for Disciplined Convex Programming*, Ver. 1.21, Apr. 2011.
- [29] J. Kim, Y. Tian, S. Mangold, and A. F. Molisch, "Quality-aware coding and relaying for 60 GHz real-time wireless video broadcasting," in *Proc. IEEE ICC*, Jun. 2013, pp. 3741–3745.



Joongheon Kim (M'06) received the B.S. and M.S. degrees from Korea University, Seoul, Korea, in 2004 and 2006, respectively. He has been pursuing the Ph.D. degree at the University of Southern California, Los Angeles, CA, USA, since 2009. He was with LG Electronics, Seoul, Korea, from 2006 to 2009. His current research interests include multi-gigabit millimeter-wave wireless systems and device-to-device distributed streaming platforms.



Yafei Tian (S'05–M'08) received the B.S. degree in electronics engineering and the Ph.D. degree in signal and information processing from Beihang University, Beijing, China, in 2001 and 2008, respectively. Since 2008, he has been a Lecturer with the School of Electronics and Information Engineering, Beihang University, where he became an Associate Professor in 2012. He was a Visiting Scholar with the University of Southern California, Los Angeles, CA, USA, from 2010 to 2011. His current research interests include wireless communications and signal processing, including next-generation cellular systems, cooperative communications, and interference management.



Stefan Mangold (M'01) received the degrees in electrical engineering and telecommunications from RWTH Aachen University, Aachen, Germany (Ph.D. degree with *summa cum laude* in 2003). He is currently a Senior Research Scientist at Disney Research, Zurich, Switzerland, where he leads the team that contributes to Disney Research's work on wireless communication and mobile computing. Before joining Disney Research in 2009, he was with Swisscom, Lausanne, Switzerland, and Philips Research, Briarcliff Manor, NY, USA. He is a co-author of two books and holds various patents and publications. His current research interests include many aspects of wireless communication networks, mainly, protocols and system aspects for IEEE 802.11 wireless LAN, visible light communication, active RFID, cognitive radios, and wide area networks such as LTE and beyond. Other research interests include interactive toys and play patterns, magic experience designs, and mobile entertainment applications. Dr. Mangold consults the European Commission as an independent expert for the research program on future networks.



Andreas F. Molisch (S'89–M'95–SM'00–F'05) received the Dipl. Ing., Ph.D., and Habilitation degrees from the Technical University of Vienna, Vienna, Austria, in 1990, 1994, and 1999, respectively.

He subsequently was with AT&T (Bell) Laboratories Research, Murray Hill, NJ, USA, Lund University, Lund, Sweden, and Mitsubishi Electric Research Laboratories, Cambridge, MA, USA. He is currently a Professor of Electrical Engineering with the University of Southern California, Los Angeles, CA, USA. He has authored, co-authored, or edited

four books (among them the textbook *Wireless Communications*, Wiley-IEEE Press), 16 book chapters, more than 150 journal papers, and numerous conference contributions, as well as more than 70 patents and 60 standards contributions. His current research interests include the measurement and modeling of mobile radio channels, ultrawideband communications and localization, cooperative communications, multiple-input multiple-output systems, and wireless systems for healthcare.

Dr. Molisch has been an Editor of a number of journals and special issues, General Chair, Technical Program Committee Chair, or Symposium Chair of multiple international conferences, as well as the Chairman of various international standardization groups. He is a fellow of the AAAS, fellow of the IET, an IEEE Distinguished Lecturer, and a member of the Austrian Academy of Sciences. He has received numerous awards, most recently the Donald Fink Prize of the IEEE and the Eric Sumner Award of the IEEE.